

Magnetoresistance of Fe₃O₄-graphene-Fe₃O₄ junctions

Zhi-Min Liao,^{1,2,a)} Han-Chun Wu,^{1,3,a)} Jing-Jing Wang,¹ Graham L. W. Cross,^{1,3} Shishir Kumar,^{1,4} Igor V. Shvets,^{1,3} and Georg S. Duesberg^{1,4,a)}

¹Centre for Research on Adaptive Nanostructures and Nanodevices (CRANN), Trinity College, Dublin 2, Ireland

²Department of Physics, State Key Laboratory for Mesoscopic Physics, Peking University, Beijing 100871, People's Republic of China

³School of Physics, Trinity College, Dublin 2, Ireland

⁴School of Chemistry, Trinity College, Dublin 2, Ireland

(Received 15 September 2010; accepted 16 January 2011; published online 3 February 2011)

The magnetoresistance (MR) of Fe₃O₄-graphene-Fe₃O₄ junctions has been experimentally studied at different temperatures. It is found that a barrier exists at the Fe₃O₄/graphene interface. The existence of the interfacial barrier was further confirmed by the nonlinear I-V characteristics and nonmetallic temperature dependence of the interfacial resistance. Moreover, spin dependent transport at the interfaces contributes -1.6% MR to the whole device at room temperature and can be regulated by an external electric field. © 2011 American Institute of Physics. [doi:10.1063/1.3552679]

Graphene is a two-dimensional (2D) material with promising applications for spintronics.¹⁻⁴ The lifetime of the spin-polarized current in graphene has been demonstrated to be very long (microsecond regime), owing to the weak spin-orbit coupling of the carbon atoms.⁵⁻⁹ Due to a high carrier Fermi velocity of 10⁶ m/s,¹ a large spin-relaxation length is also expected,¹⁰ which makes it a promising candidate for spin information transformation. Recently, many experiments have been carried out focusing on spin-valve devices by utilizing ferromagnetic metal as electrodes.^{3,11,12} As an alternative ferromagnetic material, ferromagnetic oxides are expected to be superior to metals as a spin injection source because of the existence of interfacial barriers between the oxide electrode and carbon material, which has the advantages including high spin polarization, environmental stability, and efficient spin injection.¹³ An important ferromagnetic oxide, Fe₃O₄, has been attracting tremendous attention over the past few decades. Fe₃O₄ is an archetype magnetic material with a high Curie temperature of about 850 K and is expected to have a fully spin-polarized electron band at the Fermi level, which is suitable for spintronic devices.¹⁴⁻¹⁷ Herein, we report on the fabrication and magnetoresistance (MR) properties of Fe₃O₄-graphene-Fe₃O₄ junctions. Our experimental results suggest that a barrier exists at the Fe₃O₄/graphene interface. The spin dependent transport at the interfaces was found to be sensitive to the external electric field.

Graphene flakes on a Si substrate with a 300 nm SiO₂ layer were obtained by mechanical exfoliation from the Kish graphite.¹ The desired graphene flakes were selected under an optical microscope and their positions were recorded by predefined markers on the substrate. Electrode patterns on the graphene flakes were defined by electron-beam lithography. A 50 nm Fe₃O₄ thin film was grown on the substrate via oxygen plasma assisted molecular beam epitaxy.¹⁷ Finally, Fe₃O₄-graphene-Fe₃O₄ junctions were formed after lift-off process. The magnetotransport measurements were per-

formed utilizing a physical properties measurement system (Quantum Design).

The magnetization hysteresis loop of the Fe₃O₄ thin film was shown as an inset in Fig. 1(a), which indicates the ferromagnetic nature of the Fe₃O₄ thin film at room temperature. The Raman spectra of the contacted graphene flakes were measured using a Renishaw inVia Raman microscope with a 633 nm laser excitation. A typical Raman spectrum is shown in Fig. 1(a). The two peaks located at 1585 and 2647 cm⁻¹ correspond to the G band and 2D band of bilayer graphene excited by 633 nm laser, respectively.¹⁸ The background Raman signal may be due to the existence of the

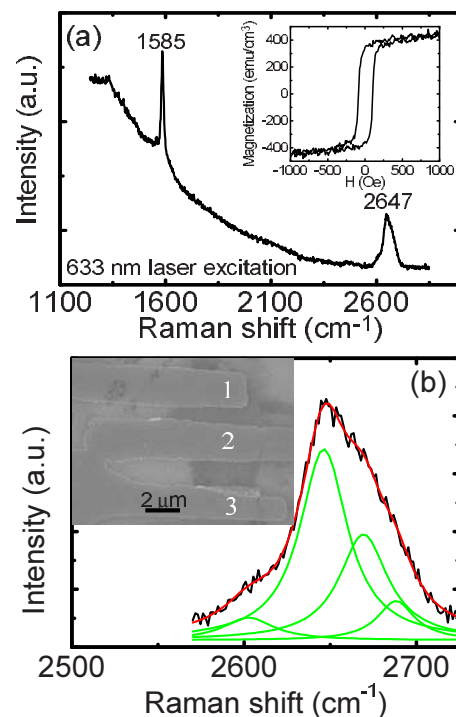


FIG. 1. (Color online) (a) Raman spectrum of the graphene sample recorded with 633 nm laser excitation. Inset: hysteresis magnetization loop of the Fe₃O₄ thin film measured at 300 K. (b) The 2D band containing four components shows that the graphene is bilayer in nature. Inset: SEM image of the Fe₃O₄-graphene-Fe₃O₄ junction.

^{a)}Authors to whom correspondence should be addressed. Electronic addresses: liaozm@pku.edu.cn, wuhc@tcd.ie, and duesberg@tcd.ie.

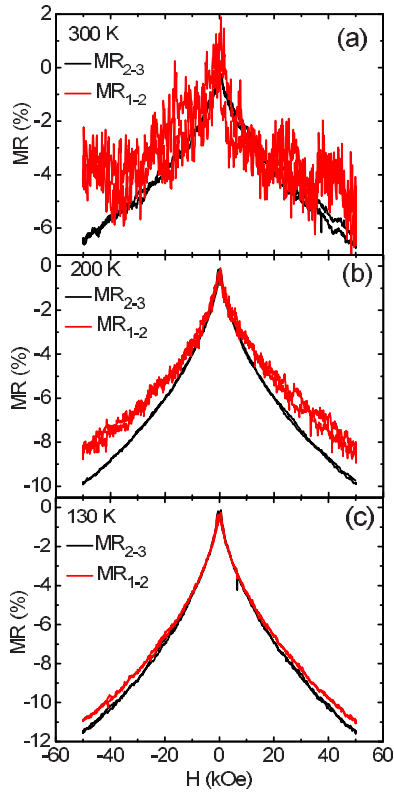


FIG. 2. (Color online) The MR measured at temperatures of (a) 300 K, (b) 200 K, and (c) 130 K. The red curves are measured by using contacts 1 and 2 and the black curves are measured by using contacts 2 and 3 as denoted by the SEM image in the inset of Fig. 1(a).

Fe_3O_4 electrodes. As shown in Fig. 1(b), a good fit of the 2D band can be made with four Lorentzian peaks, which confirms the bilayer nature of the grapheme flake.¹⁸

The inset in Fig. 1(b) is a scanning electron microscope (SEM) image of the measured junction device. The upper two Fe_3O_4 electrodes (contacts 1 and 2 as denoted) contacting the graphene sheet are separated by a distance of approximately 700 nm. The lower two Fe_3O_4 electrodes (contacts 2 and 3) are connected to each other. The MR of the Fe_3O_4 -graphene- Fe_3O_4 junction was measured using contact electrodes 1 and 2. However, the resistances of the Fe_3O_4 electrodes have a significant part in our two-probe devices. To decouple this contribution, the MR of the electrodes was measured using contacts 2 and 3.

The MRs, defined as $\text{MR} = [R(H) - R(0)]/R(0)$, measured with an in-plane magnetic field, are shown in Fig. 2. More than three devices have been measured and we got the similar results from all the devices. At 300 K, the MR of the Fe_3O_4 electrodes is $\sim -6.8\%$ with a 50 kOe magnetic field and no evidence of saturation was observed, which is attributed to the antiferromagnetic exchange coupling at the grain boundaries or the antiphase boundaries.^{14,17} The MR of Fe_3O_4 -graphene- Fe_3O_4 junction is slightly smaller than that of the Fe_3O_4 electrodes. The graphene device consists of five distinct regions, two electrodes, two interfaces, and one graphene piece. Therefore, the MR of the device can be formulated as

$$\text{MR} = \frac{2R_F(H) + R_G(H) + 2R_{F/G}(H)}{2R_F(0) + R_G(0) + 2R_{F/G}(0)} - 1, \quad (1)$$

where R_F , R_G , and $R_{F/G}$ are the resistances of the Fe_3O_4 electrodes, graphene, and interface between the Fe_3O_4 and

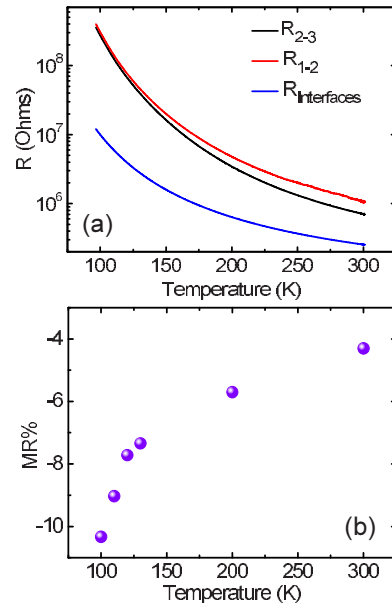


FIG. 3. (Color online) (a) The temperature dependent resistance of the electrodes, the whole junction, and the contact interfaces. (b) The temperature dependent MR of the Fe_3O_4 /graphene interfaces at a magnetic field of 5 T.

graphene, respectively. Here, R_G may lower the MR of the device as previous studies have indicated a positive MR of graphene at high magnetic fields.¹⁹ Moreover, the interface resistances also contribute to the total resistance. At 300 K, the MR_{1-2} (-6%) is slightly less than MR_{2-3} (-6.8%), as seen in Fig. 2(a). By subtracting the MR contributing from the Fe_3O_4 electrodes, one can obtain that the resistance variation from the interfaces and graphene contributes -1.6% MR to the whole junction. Nevertheless, the difference of the MR between the device and the electrodes decreases with decreasing temperature, as shown in Figs. 2(b) and 2(c), which suggests that the electrode resistance may dominate the electrical properties of the device at low temperatures. Therefore, it is worth to study the temperature dependence of the resistance. Figure 3(a) shows the temperature dependent resistances of the electrodes and the graphene device measured by applying a constant current bias of 50 nA. In order to extract the interface resistance, we first calculated the activation energy of Fe_3O_4 electrode ($E_{aF} = 71.7$ meV) by fitting the measured resistance using contacts 2 and 3 with the following formula:

$$R_{2-3}(T) = R_{F2-3} \exp(E_{aF}/k_B T). \quad (2)$$

R_{F2-3} is a constant. As the resistance of the three Fe_3O_4 electrodes should have the same activation energy, the measured resistance using contacts 1 and 2 can be written as

$$R_{1-2}(T) = R_{F1-2} \exp(E_{aF}/k_B T) + R_I \exp(E_{aI}/k_B T), \quad (3)$$

where the first term is the resistance contributing from the Fe_3O_4 electrodes and the second term is the resistance of contact interfaces. R_{F1-2} and R_I are two constants and E_{aI} is the activation energy for the Fe_3O_4 /graphene interfaces. By fitting the experimental data using Eq. (3), $R_I = 40872 \Omega$ and $E_{aI} = 47.3$ meV were obtained. The calculated resistance of the Fe_3O_4 /graphene interfaces ($R_{\text{interfaces}}$) is shown as the blue line in Fig. 3(a). $R_{\text{interfaces}}$ increased in almost two orders of magnitude as temperature decreased from 300 to 100 K. The nonmetallic temperature dependence

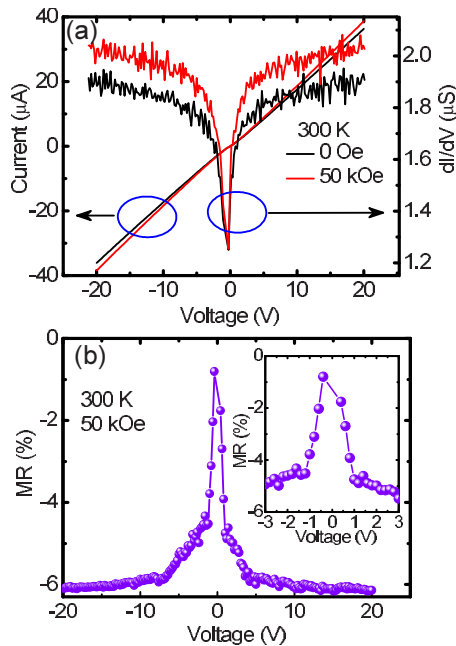


FIG. 4. (Color online) (a) dI/dV vs V and I - V curves of the Fe_3O_4 -graphene- Fe_3O_4 device measured at 300 K and with magnetic field of 0 and 50 kOe. (b) The voltage dependence of the MR under a magnetic field of 50 kOe. Inset: the magnified view of MR near zero voltage.

indicates that contact barriers exist at the interfaces.

In order to extract and estimate the spin dependent transport at the interface, we define MR of the interfaces ($\text{MR}_{F/G}$) as $\text{MR}_{F/G} = R_{F/G}(H)/R_{F/G}(0) - 1$. Since the graphene resistance is on the order of $\text{k}\Omega$ which is much smaller than the interface resistance ($\text{M}\Omega$), $R_{F/G}$ can be simply calculated by subtracting the electrodes resistance from the total resistance of the device. The temperature dependence of $\text{MR}_{F/G}$ is summarized in Fig. 3(b). It is found that $\text{MR}_{F/G}$ increases with decreasing temperature, which can be attributed to the enhanced spin polarization both in the Fe_3O_4 electrodes and graphene with decreasing temperature.

We believe that the Fe_3O_4 /graphene interfaces work as a tunnel junction¹³ and the electrical behavior of the interface meets the proper tunneling criteria.²⁰ First, there is a nonmetallic temperature dependence of interface resistance as derived above [Fig. 3(a)]. Second, the device displays nonlinear I - V curves at low bias voltage, as seen in Fig. 4(a). Third, the dI/dV vs V curves [Fig. 4(a)] show a quasiparabolic relationship. Moreover, the barrier height $\phi=0.1$ eV was estimated from the nonlinear I - V curves considering the electron tunneling model.²¹ Therefore, the significant change of $R_{F/G}$ under magnetic field may be attributed to the spin dependent tunneling at the interfaces.

The tunneling barriers also allow us to tune the MR of the junction by an external electrical field. Figure 4(b) shows the bias voltage dependent MR of the whole device at room temperature. The bias voltage dependent MR at 5 T can be written as

$$\text{MR}(V, 5 \text{ T}) = \frac{2R_F(5 \text{ T}) + R_G(5 \text{ T}) + 2R_{F/G}(V, 5 \text{ T})}{2R_F(0) + R_G(0) + 2R_{F/G}(V, 0)} - 1. \quad (4)$$

As the resistances of the electrodes and graphene are independent of the bias voltage, the bias voltage dependent MR effects are due to the modification of spin dependent transport at the interfaces. At low bias voltage, the device resistance is dominated by the spin dependent tunneling at the

interface. As the bias voltage is increased, the interface resistance decreases dramatically [see the inset of Fig. 4(b)], accordingly the resistance of the whole device decreases gradually, which therefore enhances the calculated MR. When further increasing the voltage, the interface tunneling less affects the electron transport and the total device resistance is dominated by the electrodes, which results in the saturation of MR at high bias voltage as shown in Fig. 4(b).

In conclusion, Fe_3O_4 -graphene- Fe_3O_4 junctions were fabricated. The nonlinear I - V characteristics and the nonmetallic temperature dependence of the Fe_3O_4 /graphene interface resistance indicate the existence of interfacial barriers. The MR of the interface increases with decreasing temperature. Our work shows that ferromagnetic oxide electrodes may be valuable for the realization of graphene-based spin devices operated at ambient temperature.

This work was supported by the SFI under Contracts No.06/IN.1/191, 008/IN.1/1932, and 08/CE/11432. Z.-M.L. acknowledges the support from NSFC Grant No. 10804002. S.K. acknowledges IRCSET for funding.

¹K. S. Novoselov, A. K. Geim, S. V. Morozov, D. Jiang, M. I. Katsnelson, I. V. Grigorieva, S. V. Dubonos, and A. A. Firsov, *Nature (London)* **438**, 197 (2005).

²N. Tombros, C. Jozsa, M. Popinciuc, H. T. Jonkman, and B. J. van Wees, *Nature (London)* **448**, 571 (2007).

³S. Cho, Y.-F. Chen, and M. S. Fuhrer, *Appl. Phys. Lett.* **91**, 123105 (2007).

⁴W. Han, W. H. Wang, K. Pi, K. M. McCreary, W. Bao, Y. Li, F. Miao, C. N. Lau, and R. K. Kawakami, *Phys. Rev. Lett.* **102**, 137205 (2009).

⁵K. Pi, Wei Han, K. M. McCreary, A. G. Swartz, Yan Li, and R. K. Kawakami, *Phys. Rev. Lett.* **104**, 187201 (2010).

⁶D. Huertas-Hernando, F. Guinea, and A. Brataas, *Phys. Rev. B* **74**, 155426 (2006).

⁷H. Min, J. E. Hill, N. Sinitsyn, B. Sahu, L. Kleinman, and A. H. MacDonald, *Phys. Rev. B* **74**, 165310 (2006).

⁸Y. Yao, F. Ye, X.-L. Qi, S.-C. Zhang, and Z. Fang, *Phys. Rev. B* **75**, 041401(R) (2007).

⁹D. Huertas-Hernando, F. Guinea, and A. Brataas, *Phys. Rev. Lett.* **103**, 146801 (2009).

¹⁰A. H. Castro Neto, F. Guinea, N. M. R. Peres, K. S. Novoselov, and A. K. Geim, *Rev. Mod. Phys.* **81**, 109 (2009).

¹¹E. W. Hill, A. K. Geim, K. Novoselov, F. Schedin, and P. Blake, *IEEE Trans. Magn.* **42**, 2694 (2006).

¹²W. H. Wang, K. Pi, Y. Li, Y. F. Chiang, P. Wei, J. Shi, and R. K. Kawakami, *Phys. Rev. B* **77**, 020402(R) (2008).

¹³L. E. Hueso, J. M. Pruneda, V. Ferrari, G. Burnell, J. P. Valdés-Herrera, B. D. Simons, P. B. Littlewood, E. Artacho, A. Fert, and N. D. Mathur, *Nature (London)* **445**, 410 (2007).

¹⁴H. Liu, E. Y. Jiang, H. L. Bai, R. K. Zheng, H. L. Wei, and X. X. Zhang, *Appl. Phys. Lett.* **83**, 3531 (2003).

¹⁵Z. M. Liao, Y. D. Li, J. Xu, J. M. Zhang, K. Xia, and D. P. Yu, *Nano Lett.* **6**, 1087 (2006).

¹⁶X. W. Li, A. Gupta, G. Xiao, W. Qian, and V. P. Dravid, *Appl. Phys. Lett.* **73**, 3282 (1998); P. Seneor, A. Fert, J. L. Maurice, F. Montaigne, F. Petroff, and A. Vaures, *ibid.* **74**, 4017 (1999); H. C. Wu, S. K. Arora, O. N. Mryasov, and I. V. Shvets, *ibid.* **92**, 182502 (2008).

¹⁷H. C. Wu, M. Abid, B. S. Chun, R. Ramos, O. N. Mryasov, and I. V. Shvets, *Nano Lett.* **10**, 1132 (2010).

¹⁸A. C. Ferrari, J. C. Meyer, V. Scardaci, C. Casiraghi, M. Lazzeri, F. Mauri, S. Piscanec, D. Jiang, K. S. Novoselov, S. Roth, and A. K. Geim, *Phys. Rev. Lett.* **97**, 187401 (2006).

¹⁹Y. B. Zhou, B. H. Han, Z. M. Liao, Q. Zhao, J. Xu, and D. P. Yu, *J. Chem. Phys.* **132**, 024706 (2010).

²⁰J. J. Åkerman, R. Escudero, C. Leighton, S. Kim, D. A. Rabson, R. W. Dave, J. M. Slaughter, and I. K. Schuller, *J. Magn. Magn. Mater.* **240**, 86 (2002).

²¹W. F. Brinkman, R. C. Dynes, and J. M. Rowell, *J. Appl. Phys.* **41**, 1915 (1970).